

**Electronic Supplementary Material (ESI) for Journal of Materials Chemistry B.**

**This journal is © The Royal Society of Chemistry 2018**

## Electronic Supplementary Information

### **Phototactic liquid micromotor**

Dongmei Zhang, Yunyu Sun,\* Mingtong Li, Hui Zhang,\* Bo Song, and Bin Dong\*

Institute of Functional Nano & Soft Materials (FUNSOM), Jiangsu Key Laboratory for Carbon-Based Functional Materials & Devices and Collaborative Innovation Center (CIC) of Suzhou Nano Science and Technology, Soochow University, Suzhou, Jiangsu 215123, P. R. China,

\*E-mail: [huizhang@suda.edu.cn](mailto:huizhang@suda.edu.cn), [bdong@suda.edu.cn](mailto:bdong@suda.edu.cn)

**Video S1.** The positive-phototactic motion of the liquid micromotor activated by  $0.3 \text{ W/cm}^2$  white light.

**Video S2.** The negative-phototaxis of the liquid micromotor activated by  $0.7 \text{ W/cm}^2$  white light.

**Video S3.** The motion of liquid micromotor under  $0.3 \text{ W/cm}^2$  white light in the absence of SP.

**Video S4.** The controlled movement of the liquid micromotor based on combined positive and negative phototaxis, resulting in a 'U' shaped moving trajectory.

**Video S5.** The video showing a liquid micromotor captures and transports a cargo.

**Video S6.** Two liquid micromotors approach and fuse based on the combined positive and negative phototaxis. Note that the microscopic field of view is moved to the right at 4 s.

**Video S7.** The positive (A) and negative (B) phototactic behavior of a human serum microdroplet under  $0.3$  and  $0.7 \text{ W/cm}^2$  irradiation, respectively.

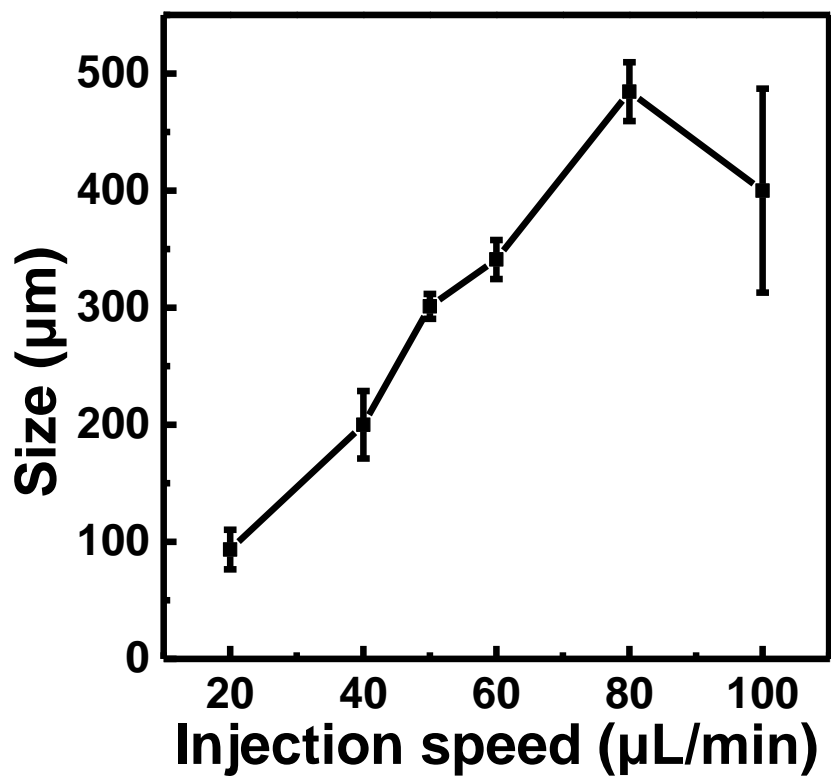


**Fig. S1** The relationship between the microdroplet size and the injection speed. The stirring speed is fixed at 500 rpm.

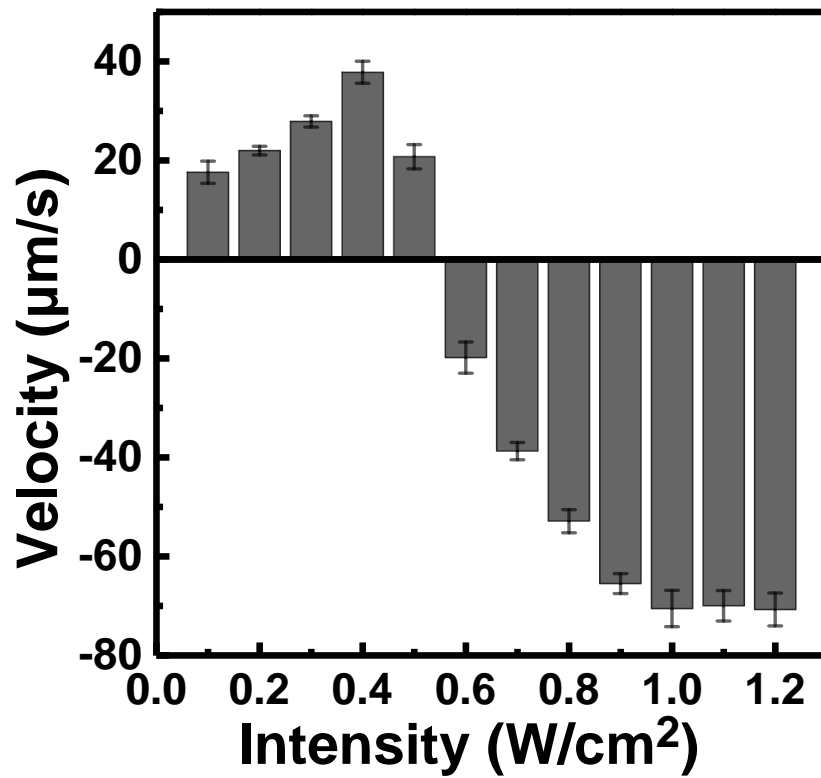


**Fig. S2** The relationship between the micromotor velocity and light intensity. Note that the speed of the negative phototaxis is defined as negative.

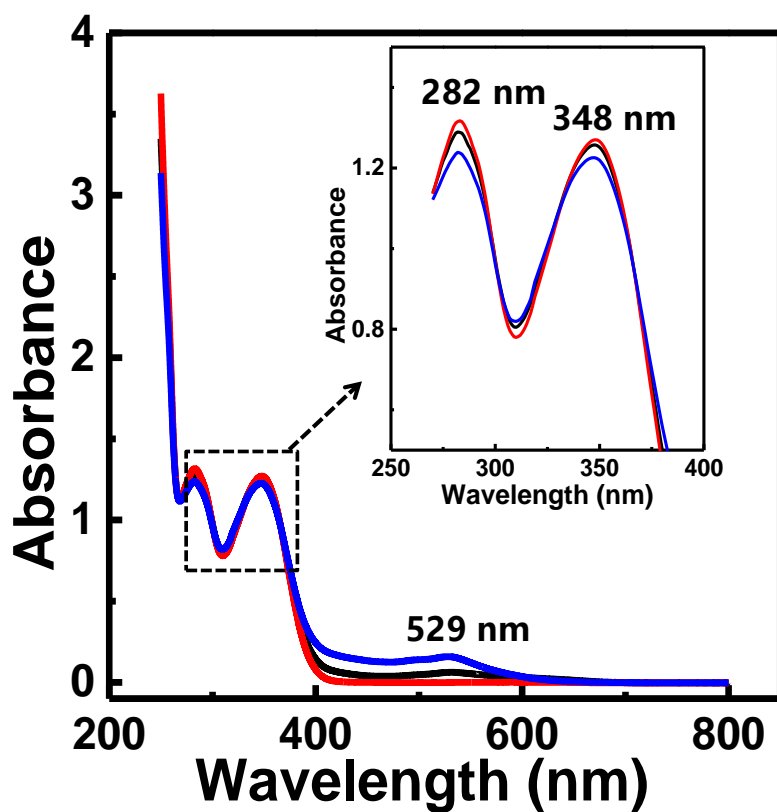


**Fig. S3** UV-Vis spectra showing the original SP molecule (red curve), after 15 s white light irradiation (blue curve) and after the white light is off for 20 min (black curve).

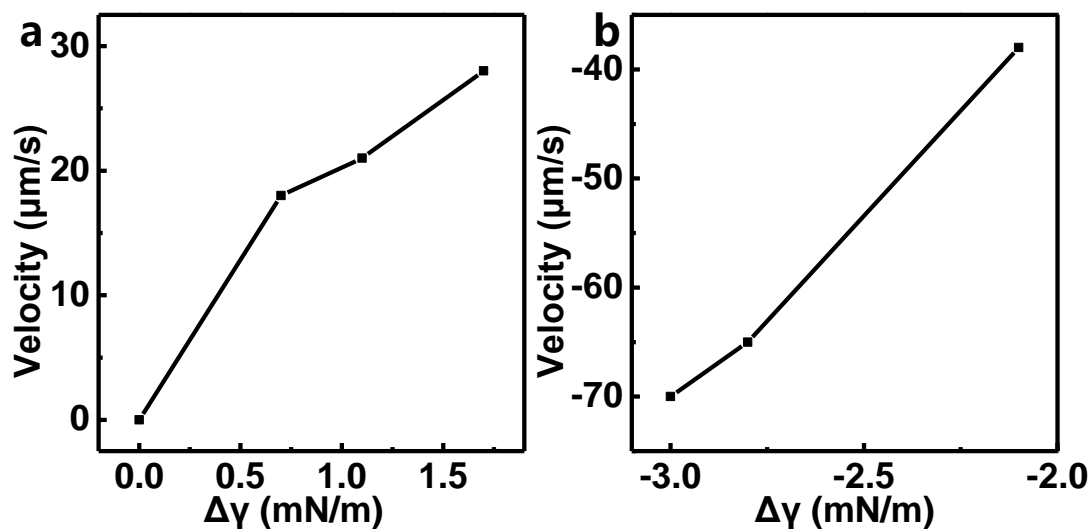


**Fig. S4** The relationship between the micromotor velocity and the interfacial tension difference in the case of (a) positive and (b) negative phototaxis. Note that the speed of the negative phototaxis is defined as negative and the interfacial tension difference ( $\Delta\gamma$ ) is the difference between values for the non-irradiated and irradiated sides.

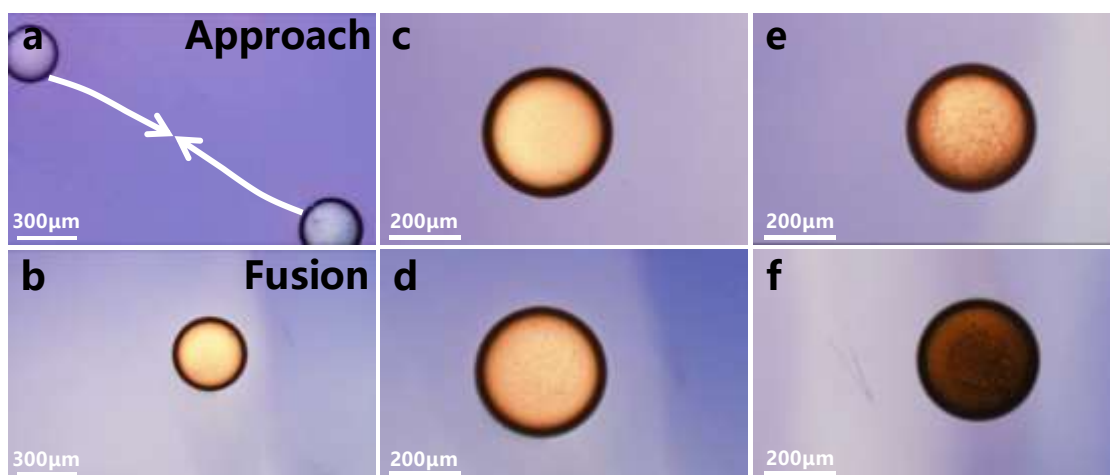


**Fig. S5** Optical microscopic images indicating (a-b) the approach and fusion between the serum microdroplets and the Fehling's solution. Glucose detection of the serum droplet containing (c) 10, (d) 50, (e) 100 and (f) 1000 mM glucose.

Based on the phototactic behavior of the biofluid-based micromotor, we have explored its potential in the field of glucose detection. As can be seen from Fig. S4a, the serum microdroplet at the upper left corner contains 5 mM glucose, while the one at the lower right corner consists of Fehling's solution (a mixture of NaOH, CuSO<sub>4</sub> and C<sub>4</sub>H<sub>4</sub>KNaO<sub>6</sub>). Fehling's solution is commonly utilized to identify glucose, which is capable of producing brick-red cuprous oxide precipitates in the presence of glucose. Under light irradiation (0.7 W/cm<sup>2</sup>), the two microdroplets move toward each other due to the combined positive and negative phototaxis. They finally contact with each other, fuse and react, leading to the formation of the characteristic brick-red precipitates (Fig. S4b), which is an indication of the presence of glucose in the serum. Moreover, since the color changes correspond in intensity to the amount of glucose in the serum (Fig. S5), we anticipate the current serum based micromotor may have potential applications in the field of glucose detection assay.